Composites: Part A 198 (2025) 109103

Contents lists available at ScienceDirect

Composites Part A

journal homepage: www.elsevier.com/locate/compositesa

Enhancing polypropylene/high-density polyethylene blend performance through the incorporation of microcrystalline cellulose-based core-shell particles at the interface

Ke Zhan [a,*], Yucheng Peng [a], Thomas Elder [b]

[a] College of Forestry, Wildlife and Environment, Auburn University, Auburn, AL 36849, USA
[b] Southern Research Station, USDA-Forest Service, 521 Devall Drive, Auburn, AL 36849, USA

HIGHLIGHTS

- Microcrystalline cellulose (MCC) enhanced the PP/HDPE blend's strength, stiffness, and toughness.
- Mechanical performance of the PP/HDPE blend further improved after MAPE compatibilization.
- MCC-based core-shell particles formed at the PP/HDPE interface.
- Thermal analysis revealed MCC nucleation and MAPE isolation effects.
- Rheological behavior showed percolation effects at high MCC content.

GRAPHICAL ABSTRACT

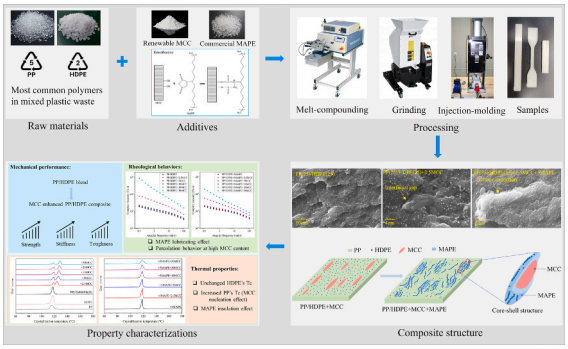

ARTICLE INFO

Keywords:
Polypropylene
High-density polyethylene
Microcrystalline cellulose
Compatibilization

ABSTRACT

Enhancing the performance of polypropylene (PP)/high-density polyethylene (HDPE) blends is crucial for valorizing mixed plastic waste. This study incorporated microcrystalline cellulose (MCC), combined with maleic anhydride grafted polyethylene (MAPE), into a PP/HDPE blend to enhance its performance. Mechanical results showed that the addition of MCC increased strength, stiffness, and toughness of the PP/HDPE blend, with further enhancement achieved through adding MAPE. Morphological observations and thermal analyses revealed that the enhanced mechanical properties were attributed to the formation of core–shell structured particles, with MCC as the core and MAPE, miscible with HDPE, acting as the shell at the interface. Rheological behaviors provided insights into processability and MCC-polymer matrix interactions of the composites, highlighting percolation effects at high MCC content. These MCC-based core–shell particles demonstrated great potential for improving the PP/HDPE blend performance.

* Corresponding author.
E-mail address: kzz0030@auburn.edu (K. Zhan).

https://doi.org/10.1016/j.compositesa.2025.109103
Received 18 April 2025; Received in revised form 30 May 2025; Accepted 7 June 2025
Available online 10 June 2025

1. Introduction

Plastics have been continuously produced since 1950 and utilized across various fields, including construction, automotive, packaging, agriculture, and medicine, owing to their lightweight, low cost, easy processability, and versatile properties [1–3]. The wide applications of plastics have led to an overwhelming amount of plastic waste, threatening ecosystems and human health [4,5]. These plastic wastes accumulate in landfills, causing economic losses, and are incinerated with risks of hazardous emissions and environmental contamination [6–8].

Globally, over 9200 million metric tons of plastics have been produced to date, with more than 70 % of waste plastics remaining unrecycled due to inefficient and energy-intensive recycling technologies [9,10]. Polyolefins, accounting for 57 % of global plastic production, generate over 220 million tons annually and are expected to quadruple by 2050 [11]. The most widely used polymers in the polyolefin family are polypropylene (PP) and polyethylene (PE), with PP and high-density PE (HDPE) primarily utilized for rigid products, and low-density PE (LDPE) and linear LDPE (LLDPE) for flexible packaging [12–14]. Their global recycling rates are extremely low, with approximately 10 % for HDPE, 6 % for LDPE and LLDPE, and only 1 % for PP, emphasizing the urgent need for sustainable waste management and more efficient recycling strategies [15].

In practical recycling scenarios, post-consumer plastics are often physically mixed and include complex materials like multilayer packaging, making polymer isolation costly and labor-intensive due to the need for advanced sorting technologies and sophisticated equipment [16]. This situation is particularly pronounced for PP and HDPE, given their similar applications, density, and chemical properties [17]. Transforming mixed plastic waste into value-added products without sorting offers a more practical, cost-effective solution that could significantly enhance plastic reclamation [16]. Direct melt-compounding of mixed plastics has emerged as a promising approach, as it eliminates the need to separate individual polymers and enables the creation of materials that combine their functions [18,19]. Therefore, PP and HDPE have been extensively studied and utilized in the form of blends through direct melt-compounding over the past decades [20–30].

However, PP and HDPE are thermodynamically immiscible due to the positive Gibbs free energy of mixing, which creates high interfacial tension between the phases [31–33]. This immiscibility promotes coalescence in the dispersed phases, causing non-uniform dispersion and phase separation during melt-compounding and crystallization. Consequently, the mechanical performance of the final PP/HDPE blend is poor, with weak stress transfer ability, ultimately limiting the blend applications to low-value-added products [28,32,34,35]. To valorize mixed plastic waste into value-added products, enhancing the mechanical performance of the PP/HDPE blend has been a long-standing focus in both research and industry.

Numerous strategies have been developed to achieve this purpose, with adding compatibilizers being widely recognized as one of the most promising approaches [25,36–40]. Compatibilizers are generally categorized as non-reactive or reactive. Non-reactive compatibilizers, such as PE-graft-PP copolymer [18], PE-block-PP copolymer [7,41], ethylene propylene rubber [13,42], ethylene propylene diene monomer (EPDM) [43,44], olefin block copolymer [13,45], and styrene-ethylene-butylene-styrene triblock copolymer (SEBS) [13], have been investigated and shown to improve the mechanical properties of PP/HDPE blends. Reactive compatibilizers, including maleic anhydride (MA) grafted PP (MAPP) [23,46,47], MA-grafted PE (MAPE) [23,37,48], MA-grafted SEBS [49], and MA-grafted EPDM [49,50], have also been studied, with MAPP and MAPE emerging as the most promising due to their commercial availability, ease of production, and effectiveness in improving phase compatibility in polymer blends. However, both types of compatibilizers have limitations. Non-reactive compatibilizers improve tensile elongation and impact strength but often reduce tensile strength and modulus. Reactive compatibilizers are less complex, cost-effective, and better at stabilizing morphology, but their improvements in toughness and stiffness are limited. A highly effective strategy to enhance mechanical performance is the simultaneous incorporation of reinforcement and a reactive compatibilizer [38,51].

Several reinforcing materials, such as clay [52–54], calcium carbonate [39,55], and wood fiber (WF) [34,50,56–58], are commonly studied in enhancing PP/HDPE blends. Among them, bio-derived reinforcements combined with compatibilizers offer desirable mechanical properties while being renewable and eco-friendly, presenting a unique opportunity for sustainable polymer composites. For instance, Clemons's study [50] demonstrated a synergistic effect in the PP/HDPE blend by adding WF and 3 wt% MAPP compatibilizer, forming strong interactions that significantly improved strength, stiffness, and toughness. A similar combined effect of WF and reactive compatibilizers was also observed in Gao et al.'s research [56].

While WF has been studied to some extent, celluloses, including cellulose nanocrystals (CNC), cellulose nanofibrils (CNF), and microcrystalline cellulose (MCC), have received extremely limited attention for enhancing PP/HDPE blends, despite their proven effectiveness in improving the mechanical properties of individual PP and HDPE [59–65]. MCC is a promising choice compared to CNC and CNF, which involve higher production costs and intricate processing, and WF, which introduces impurities and compromises the visual quality of composites. To the best of our knowledge, using MCC to enhance immiscible PP/HDPE blends remains unexplored.

In this study, MCC particles and the MAPE compatibilizer were introduced into a PP/HDPE blend (75/25 weight ratio) via melt-compounding. The mechanical, morphological, and thermal properties of the blend, enhanced by varying MCC contents and/or 5 wt% MAPE, were thoroughly examined. The objective was to explore the potential of MCC particles in improving the performance of the immiscible PP/HDPE blend with MAPE as a compatibilizer, thereby expanding the applications of biobased MCC and contributing to the valorization of mixed plastic waste.

2. Materials and methods

2.1. Materials

The PP and HDPE pellets were supplied by ExxonMobil Chemical Company (PP1024, Houston, TX, US) and Dow Chemical Company (HDPE 8920, Baytown, TX, US), respectively. The densities of PP and HDPE are 0.900 and 0.954 g/cm^3, respectively, while the melt index of PP is 13 g/10 min at 230 °C/2.16 kg and HDPE is 20 g/10 min at 190 °C/2.16 kg. MAPE was purchased from SI Group Inc. (Polybond 3009, Schenectady, NY, US), having a density of 0.950 g/cm^3 and a melt index of 5 g/10 min at 190 °C/2.16 kg, with a maleic anhydride content of 0.8 to 1.2 %. MCC particles were purchased from EMD Millipore Corporation (Burlington, MA, US). All materials were dried overnight at 105 °C to eliminate moisture before use.

2.2. Sample preparation

The PP/HDPE blend composites were prepared using an internal mixer (Model 2128, C.W. Brabender Instruments, Inc., Hackensack, NJ, US) equipped with two counter-rotating roller blades. PP and HDPE, in a weight ratio of 75/25, were added to the mixer and compounded at 200 °C and 60 rpm for 5 min. Subsequently, 5 wt% MAPE was introduced and compounded for an additional 3 min. MCC particles, at concentrations of 2.5, 5, 10, 20, and 30 wt%, were gradually added into the mixing chamber within 2 min followed by 8 min of further compounding. After compounding, the composites were solidified at room temperature and ground into particles using a low-speed granulator (Model SG-2042NH, Shini Plastic Technologies, Inc., Willoughby, OH, US) equipped with a 3 mm sieve. The particles were then dried overnight at 105 °C in an oven before injection molding. ASTM-standard mechanical testing specimens

were produced at 200 °C and 51 MPa using a benchtop injection molding machine (Proto-Ject 150 HP, Manning Innovations, Inc., Halls, TN, US) with customized aluminum molds. Sheets with a thickness of 1.5 mm were specifically produced for rheological measurements. For comparison, neat PP, neat HDPE, the unmodified PP/HDPE blend, and PP/HDPE blends containing only MCC were also prepared using the same procedure. All samples were stored in Ziploc bags after injection molding to prevent moisture adsorption before characterization.

2.3. Characterizations

2.3.1. Mechanical tests

Tensile testing was conducted according to ASTM D638 (Type IV) using a universal testing machine (Model F1505, Mark-10, Copiague, NY, US) with a 1000-N load cell and an Epsilon extensometer (Model SN E109112, Jackson, WY, US) to determine strain. The testing speed and initial strain rate were 5 mm/min and 0.1 min^{-1}, respectively. Flexural testing was performed according to ASTM D790 using a universal testing machine (Model ESM750S, Mark-10, Copiague, NY, US) equipped with a 500-N load cell, a 50 mm support span, and a crosshead motion speed of 1.34 mm/min, with flexural strength reported at 5 % strain. Impact strength was evaluated according to ASTM D256 using an XJUD Digital Charpy Izod impact tester (Deli Group Co. Ltd., Ningbo, China). Five replicates were tested for tensile and flexural tests, while ten replicates were tested for impact tests. One-way analysis of variance (ANOVA) was performed using IBM SPSS software with a significance level of $\alpha = 0.05$, followed by Tukey's Honestly Significant Difference post-hoc test to assess differences within factor groups.

2.3.2. Particle size distribution measurement

The particle size of the MCC sample was measured using a Mastersizer 2000 particle size analyzer (Malvern Instruments, Malvern, UK), following a procedure published in a previous study [61]. A Sirocco 2000 dry dispersion unit was used for the analysis. Measurements were performed at an air pressure of 4 bars and 20 % feeder capacity. Three replicates were taken for each sample.

2.3.3. Scanning electron microscopy

The morphologies of MCC particles were examined using a scanning electron microscope (SEM, EVO 50, Zeiss, Oberkochen, Germany) at an accelerating voltage of 20 kV. Samples were sputter-coated with gold for 120 s in a sputter-coating device (Q150R, Electron Microscopy Sciences, Hatfield, PA, US) to enhance conductivity. The fractured surfaces of the impact testing specimens were characterized using the same SEM method.

2.3.4. Differential scanning calorimetry

The melting and crystallization behaviors of PP, HDPE, the PP/HDPE blend, and enhanced blends were analyzed using a differential scanning calorimeter (DSC, Q20, TA Instruments, New Castle, DE, US). Samples (7–9 mg) were tested under nitrogen with a flow rate of 50 mL/min. The samples were heated from 40 °C to 200 °C at 10 °C/min, held isothermally for 5 min to erase thermal history, cooled to 40 °C at 5 °C/min to record crystallization data, and then reheated to 200 °C at 10 °C/min to observe melting behavior. The crystallization peak temperature (T_c) was determined from the cooling scan, whereas the melting peak temperature (T_m) and enthalpy were derived from the second heating scan. The degree of crystallinity (X_c) was calculated according to the following equation [66]:

$$X_c(\%) = \frac{1}{wt.\%}\left[\frac{\Delta H_m}{\Delta H_{m0}}\right] \times 100$$

where ΔH_m is the melting enthalpy of PP or HDPE; ΔH_{m0} is the melting enthalpy for a 100 % crystalline PP or HDPE; and *wt.%* represents the weight fraction of the individual PP or HDPE component in the blends. The ΔH_{m0} for a 100 % crystalline PP was 205 J/g [67], while the value of ΔH_{m0} for 100 % crystalline PE was assumed to be 290 J/g [68].

2.3.5. Rheological measurements

Rheological properties were investigated using a rheometer (HAAKE MARS 60, Thermo Fisher Scientific, Germany) equipped with a parallel plate geometry (diameter = 25 mm, gap = 1.3 mm). The circular specimens with a diameter of 22 mm and a thickness of 1.5 mm were prepared from the injection-molded sheets using a Gasket punch (General Tools, Cincinnati, OH, US). The linear viscoelastic regions (LVR) were determined by oscillation strain sweeps (0.05–350 %) at a constant angular frequency of 6.283 rad/s. Frequency sweeps were performed over an angular frequency range from 0.1 to 100 rad/s within LVR to obtain viscoelastic properties as functions of frequency, including complex viscosity (η*), storage modulus (G'), loss modulus (G"), and Tan delta (Tan δ). For the creep-recovery test, a constant stress of 50 Pa was applied. The strain as a function of time was recorded in the first 300 s for the creep stage, while the strain as a function of time was recorded in the latter 500 s for the recovery stage. All data were averaged over three replicates with error bars to indicate standard deviation.

3. Results and discussion

3.1. Mechanical properties

3.1.1. Tensile and flexural properties

The tensile properties of all the composites are shown in Fig. 1 a and b. The tensile strength of the PP/HDPE blend was initially 27.4 MPa and increased significantly to 29.8 MPa with the addition of 2.5 wt% MCC, as the rigid MCC particles effectively reinforced the matrix by resisting deformation under load. However, as the MCC content increased, the tensile strength slightly decreased at 5 wt% MCC, primarily due to the incompatibility between the hydrophilic MCC and the hydrophobic PP/HDPE matrix, which created interfacial boundaries and hindered effective load transfer. The tensile strength significantly declined at MCC contents above 10 wt% and dropped to 24.3 MPa at 30 wt% MCC. This decline is attributed to the formation of agglomerates caused by poor dispersion, resulting in severe stress concentrations within the composite [63].

With the addition of MAPE alone, the tensile strength of the PP/HDPE blend increased to 29.8 MPa, having the same value observed in the blend enhanced with only 2.5 wt% MCC, as depicted with the red dotted line in Fig. 1. This improvement is attributed to the migration and interfacial localization of MAPE at the PP/HDPE boundary during high-temperature melt mixing, which enhanced compatibility and facilitated stress transfer [25,37]. When both MCC and MAPE were added, tensile strength increased further, particularly above 20 wt% MCC, reaching 32.5 MPa at 30 wt%, due to the esterification reaction between MCC's hydroxyl groups and MAPE's anhydride groups [69]. The tensile modulus of elasticity (MOE) increased consistently with increasing MCC content, regardless of MAPE presence, indicating enhanced composite stiffness due to the inherent rigidity of MCC, which limited the chain mobility of the polymer matrix under stress.

The contributions of MCC and MAPE to enhancing strength and stiffness were also observed in the flexural test, as shown in Fig. 1 c and d. For blends with high MCC content (20 wt% and 30 wt%), the addition of MAPE resulted in a notable improvement in flexural strength, as depicted by the red dotted line. It is worth noting that, unlike the tensile strength results, the flexural strength did not decrease due to the incompatibility when only MCC was added. This is attributed to the high aspect ratio of MCC particles, which tended to align parallel to the mold filling direction near the specimen surface during injection molding, enhancing resistance against the tensile forces applied to the sample's lower surface during flexural testing [70].

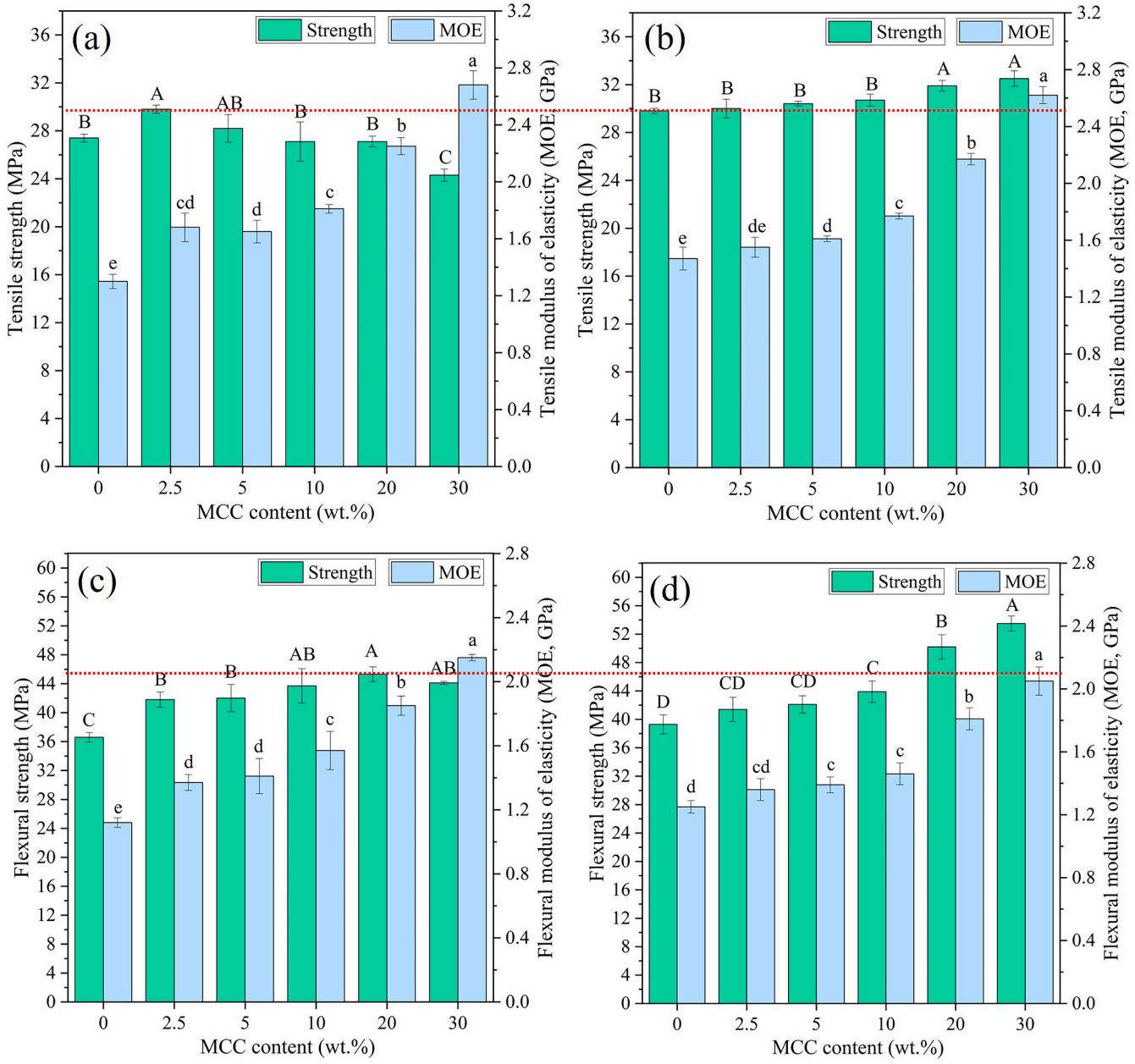

Fig. 1. Tensile and flexural properties of PP/HDPE blends enhanced with (a, c) MCC and (b, d) MCC and 5 wt% MAPE. Different letters A-D and a-d in the figures indicate statistically different groups for the strength and MOE results, respectively.

3.1.2. *Impact strength*

The impact strength, presented in Fig. 2, was measured to assess the composite's toughness. The PP/HDPE blend's impact strength increased from 1.62 kJ/m^2 to 1.85 kJ/m^2 with 2.5 wt% MCC and further to 2.06 kJ/m^2 at 5 wt% MCC, subsequently remaining relatively constant up to 30 wt% MCC. This initial enhancement is driven by MCC particles acting as effective toughening agents to absorb impact energy. However, further improvements were restricted due to incompatibility at higher MCC content.

With MAPE compatibilization alone, the impact strength of the PP/HDPE blend increased to 2.00 kJ/m^2. The addition of both 2.5 wt% MCC and MAPE further increased the impact strength to 2.41 kJ/m2, attributed to enhanced interfacial adhesion facilitated by MAPE. However, at higher MCC content, the formation of more stiff regions disrupted the polymer matrix continuity and reduced flexibility. This hindered efficient energy dissipation and counteracted MAPE's effect, thereby preventing any further significant improvement in toughness [63].

3.2. *Morphologies*

The fractured surfaces of the blends are shown in Fig. 3. PP exhibited a smooth, brittle fracture surface, while HDPE displayed a rough, ductile fracture. In the PP/HDPE blend, HDPE domains were well distributed within the PP matrix, and this distribution remained largely unchanged after MAPE compatibilization. However, under high magnification, distinct interfacial boundaries were visible in the unmodified blend (Fig. 3e), whereas MAPE compatibilization caused HDPE domains to appear bonded to the PP matrix (Fig. 3f). This enhanced compatibility is attributed to the interfacial localization of MAPE at the PP/HDPE interface during melt compounding, driven by thermodynamic forces, as discussed in the tensile strength results.

The particle size distribution and morphologies of MCC particles are shown in Fig. 4. Percentages of 10 %, 50 %, and 90 % of the particles had sizes smaller than 5.1, 15, and 39 μm, respectively. The SEM image showed that the MCC particles had a fibrous shape with a relatively high

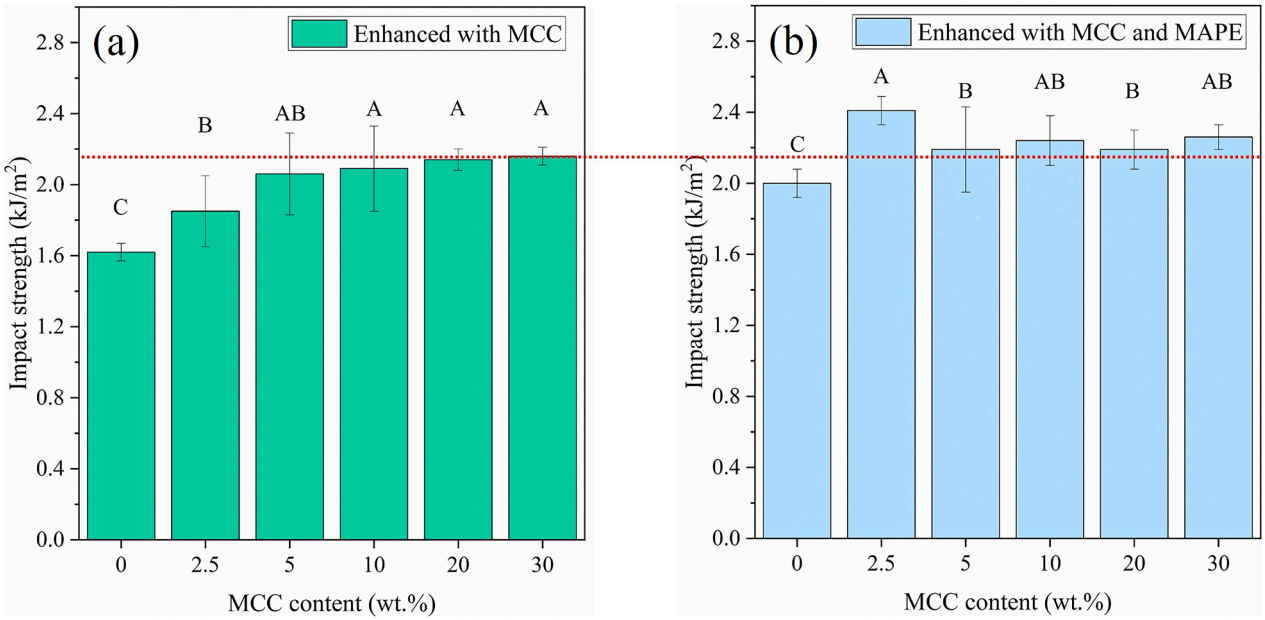

Fig. 2. Impact strength of PP/HDPE blends enhanced with (a) MCC and (b) MCC and 5 wt% MAPE.

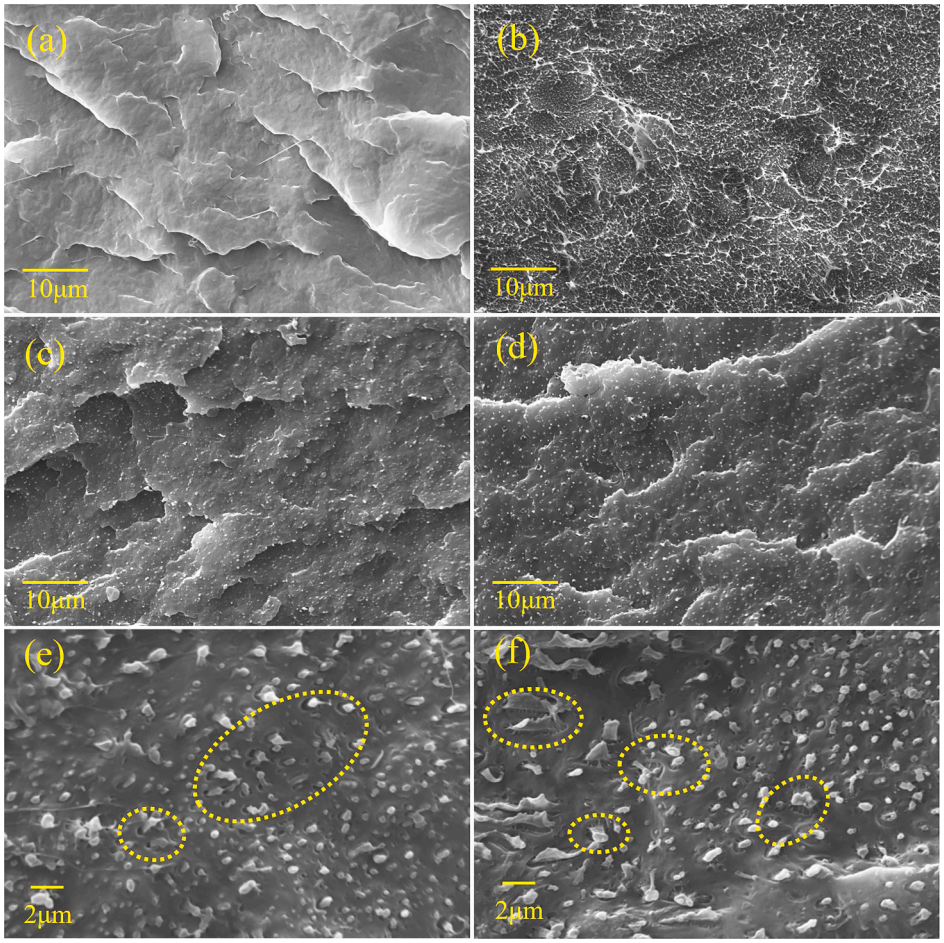

Fig. 3. SEM images of (a) PP, (b) HDPE, (c) PP/HDPE blend, (d) PP/HDPE blend with 5 wt% MAPE, (e) PP/HDPE blend under high-magnification, and (f) PP/HDPE blend with 5 wt% MAPE under high-magnification.

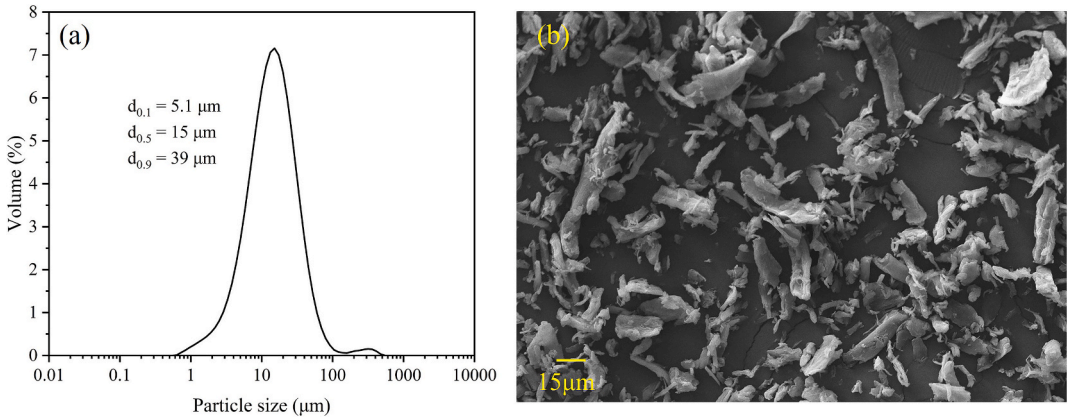

Fig. 4. (a) Morphologies and (b) particle size distribution of MCC.

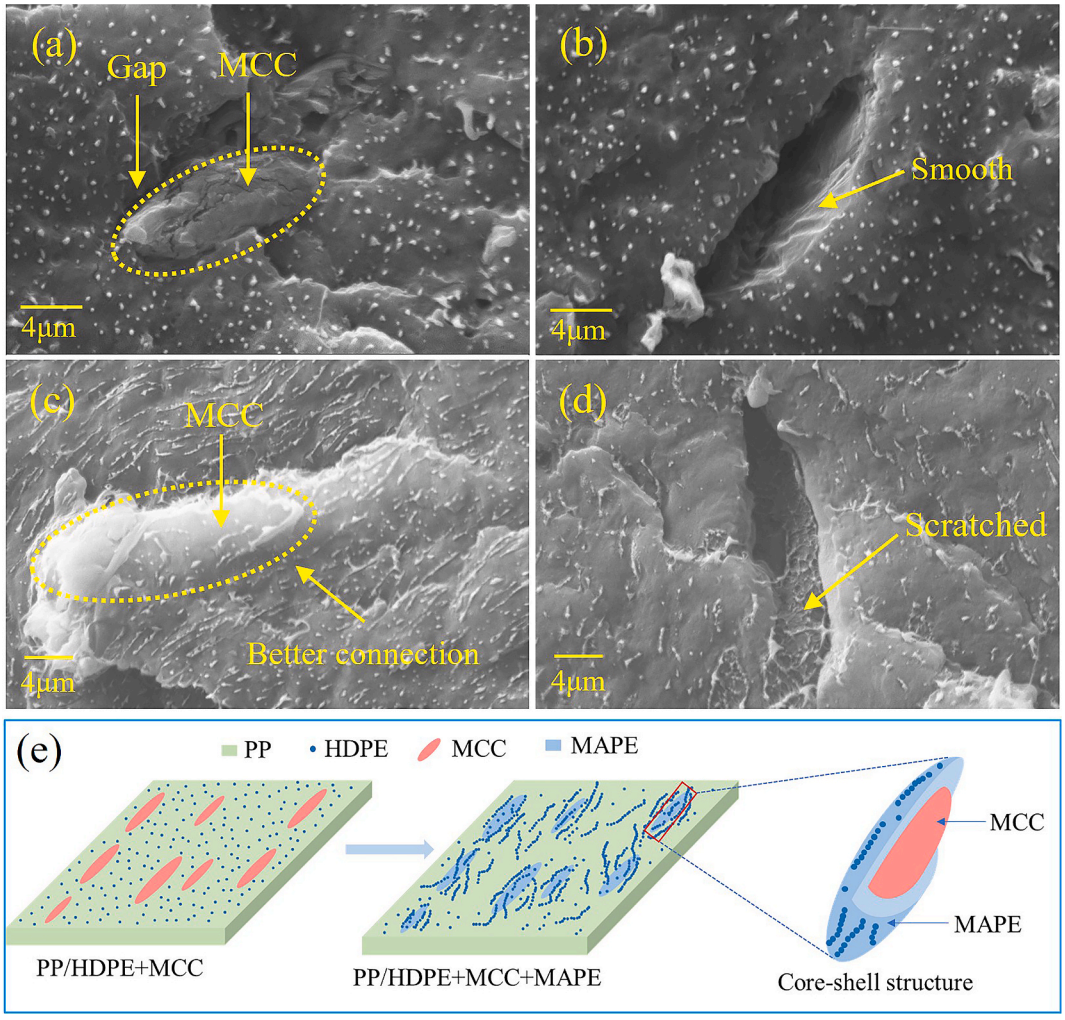

Fig. 5. SEM images of (a, b) PP/HDPE blend enhanced with 2.5 wt% MCC and (c, d) PP/HDPE blend with 2.5 wt% MCC and 5 wt% MAPE. (e) Simplified diagram of the MCC-based core–shell structure.

aspect ratio and a broad size range. The fractured surfaces of the blends enhanced with MCC are shown in Fig. 5. The incorporation of MCC alone did not significantly alter the distribution of HDPE domains. A clear gap between the polymer matrix and the MCC particle was observed in Fig. 5a, with no HDPE domains visible on the MCC particle. Fig. 5b shows a smooth, scratch-free fracture surface left after MCC removal, suggesting that the stress required to pull the MCC particle did not substantially deform the polymer matrix. These observations indicate weak interfacial adhesion and limited interaction between MCC and the PP/HDPE blend.

In contrast, with the introduction of MAPE, the interfacial gap became less distinct, as shown in Fig. 5c, where the MCC particle appeared to be wrapped by the polymer, and partial HDPE domains aligned within the PP matrix and attached to the MCC particle through

MAPE. Fig. 5d displays a rough, scratched fracture surface after MCC removal, likely resulting from the force needed to pull the particle. These features suggest enhanced interfacial adhesion and stable interactions between MCC and the PP/HDPE blend. This alteration is likely due to esterification reactions, as discussed in the results of the tensile property.

A simplified diagram in Fig. 5e illustrates the mechanism for enhancing the PP/HDPE blend's performance. During melt-compounding, the anhydride groups of MAPE reacted with the hydroxyl groups on the MCC particles, causing MAPE to encapsulate the hydrophilic MCC particles. The PE backbone of MAPE, with its high miscibility to HDPE, influenced the distribution of HDPE phases, causing HDPE domains to migrate toward the MAPE-encapsulated MCC particles and enable some to be attached to the MCC particle through MAPE. A core–shell structure was formed through this synergistic effect, where the rigid MCC particle acted as the core, contributing to improved strength and stiffness, while MAPE served as the shell, addressing the incompatibility issue between the hydrophilic MCC and the hydrophobic polymer matrix, consequently ensuring enhanced overall mechanical performance.

3.3. Thermal properties

3.3.1. Melting and crystallization behaviors

The melting and crystallization curves of PP, HDPE, the PP/HDPE blend and all composites are presented in Fig. 6. The melting peak temperatures (T_m) of neat PP and HDPE were 162.7 °C and 131.2 °C, respectively. In the PP/HDPE blend, the T_m of both PP and HDPE changed by less than 1 °C, indicating negligible mutual influence on crystalline structures. Incorporating MCC did not significantly affect the T_m of HDPE, likely due to limited direct contact, as shown in the SEM image (Fig. 5a). However, the T_m of PP increased with higher MCC content, attributed to MCC's nucleation effect, which promoted the development of well-organized and thermodynamically stable crystalline structures [69]. After MAPE compatibilization, the T_m of both PP and HDPE remained largely unaffected, as MCC's impact on polymer properties was isolated by the encapsulating MAPE.

The crystallization peak temperatures (Tc) of neat PP and HDPE were 115.8 °C and 117.8 °C, respectively. In the PP/HDPE blend, the crystallization peaks merged at 117.6 °C due to the nucleation effect of HDPE on the PP matrix, which led to a slight increase in PP's crystallization temperature [71]. Adding MAPE alone in the blend made this merged Tc shift slightly further to a higher temperature. The presence of MAPE enhanced interfacial interactions, reduced phase separation, and created more well-defined interfaces, facilitating efficient polymer chain packing within the blend. Similar to the melting behaviors, adding MCC alone did not change HDPE's Tc. At the same time, the nucleation effect of MCC lowered the energy barrier for PP's crystallization initiation and increased Tc, consequently leading to the separation of PP's and HDPE's crystallization peaks, with higher MCC content resulting in a higher Tc of PP [65]. When both MCC and MAPE were added, the crystallization peak of the composite returned to a single peak for all MCC contents, and Tc remained comparable to that of the blend modified with MAPE alone due to the isolation effect of the MAPE. The melting and crystallization analyses further confirmed the formation of the proposed core–shell structure.

More interestingly, as shown in Fig. 7, the increasing trend of Tc due to the nucleation effect with increasing MCC content was well-fitted by

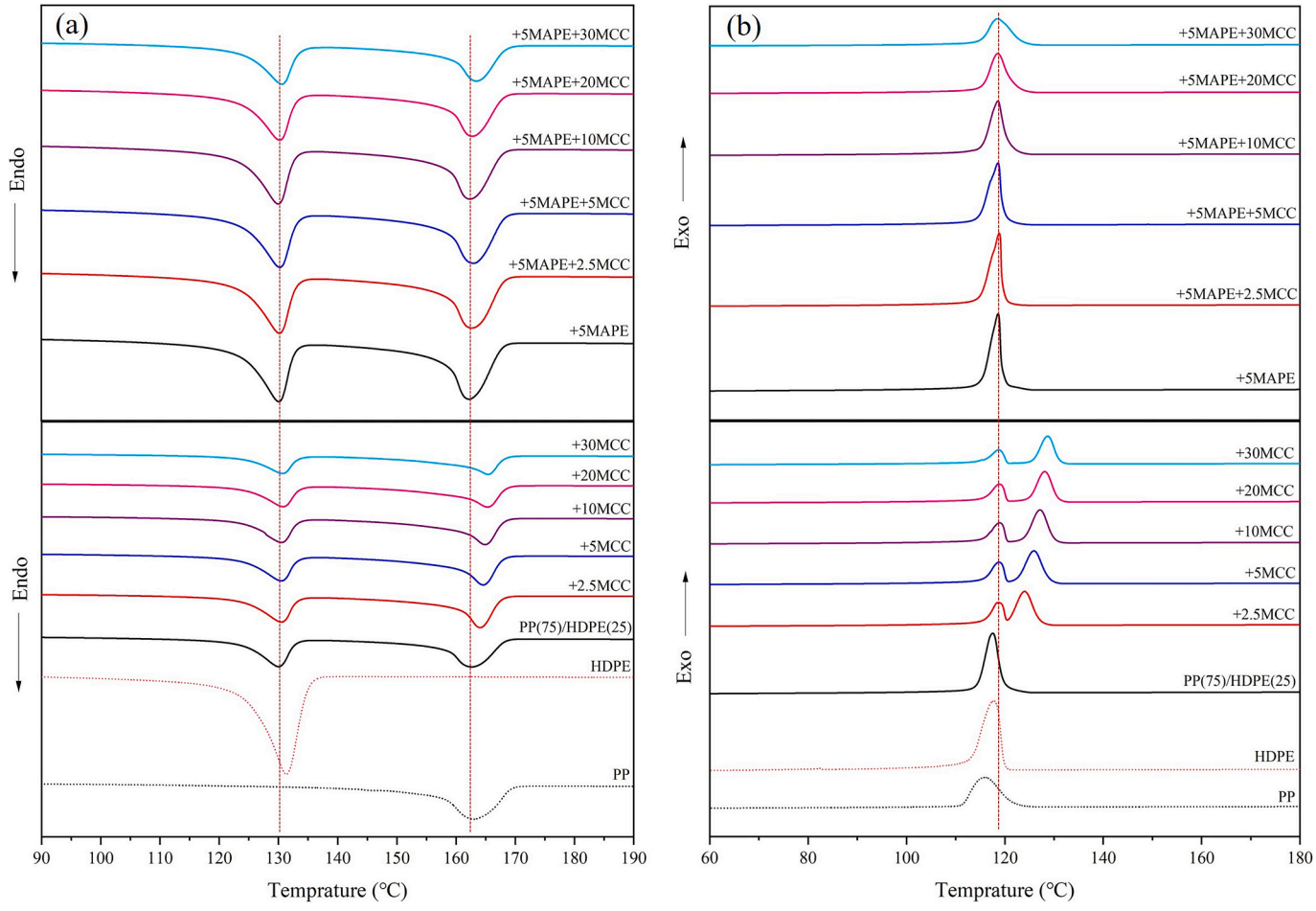

Fig. 6. (a) Melting and (b) crystallization curves of PP, HDPE, the PP/HDPE blend, and all composites.

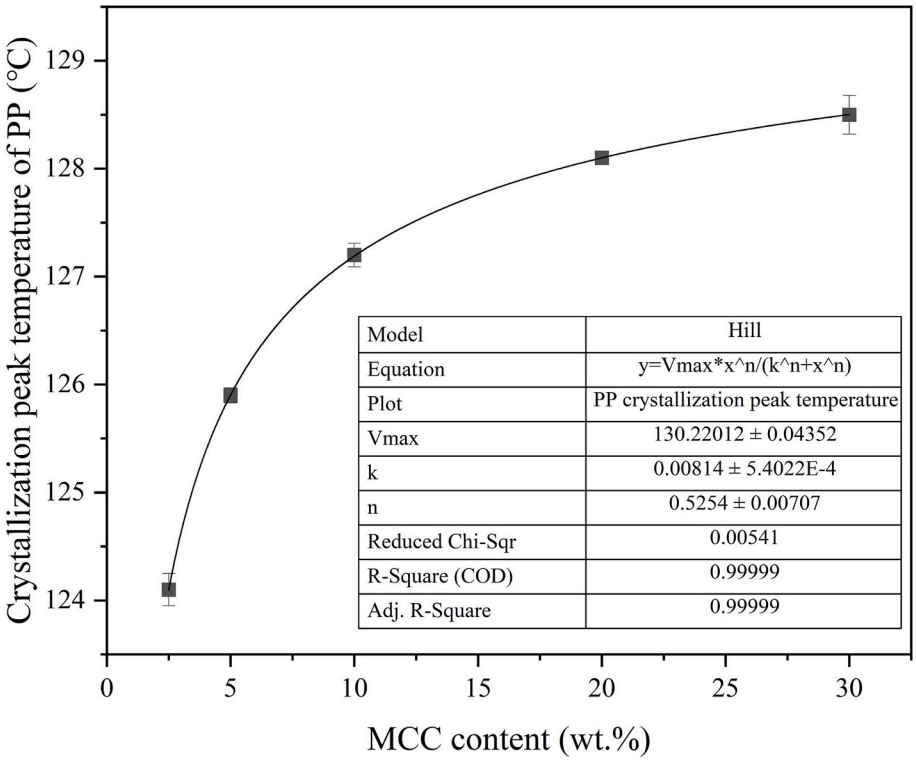

Fig. 7. The crystallization peak temperature of PP as a function of MCC content.

the Hill model, which was initially developed in biochemistry to describe the saturation behavior of ligand binding to macromolecules and is also commonly used in pharmacology to study the drug concentration saturation behavior [72,73]. Specifically, the Hill coefficient (n = 0.5254) indicates a negative cooperativity effect, suggesting that MCC particles were highly effective at lower concentrations but became less effective as the number of available nucleating sites decreased with increasing MCC content. This model may help determine the maximum effective MCC content at the plateau initiation point where saturation occurs. Beyond this point, excessive MCC leads to severe agglomeration, which no longer enhances composite performance.

However, further investigation is needed to explore the feasibility of this model or alternative models in describing the saturation behavior of the MCC particles in polymer composites. More deeply, dispersing agents or surface modifications also deserve further exploration to improve MCC dispersion and bring the n value closer to 1, where particles are perfectly dispersed without agglomeration. This approach presents a potential new avenue for predicting the optimal additive concentration while minimizing unnecessary costs in engineering polymer composite research.

3.3.2. *Crystallinity*

Fig. 8 presents the crystallinity (Xc) variations of PP and HDPE in the PP/HDPE blend and its composites. The Xc of PP showed a negligible reduction to 41.3 % in the blend, while HDPE's Xc remarkably decreased to 53.8 %, compared to neat PP (42.2 %) and neat HDPE (58.0 %). This difference is attributed to the phase morphology of the blend. The continuous PP matrix remained largely unaffected as most PP chains are distant from the PP/HDPE interface, allowing crystallization with minimal interference. In contrast, HDPE, as the dispersed phase, was confined within small droplets, restricting chain mobility and hindering ordered crystallization.

Compared to the Xc of PP and HDPE in the unmodified PP/HDPE blend, the incorporation of MCC particles (2.5, 5, and 10 wt%) had minimal impact on Xc. However, when MCC content increased to 20 wt %, Xc began to decline. This reduction can be attributed to the higher MCC content hindering polymer chain alignment and restricting the formation of ordered crystalline structures [74].

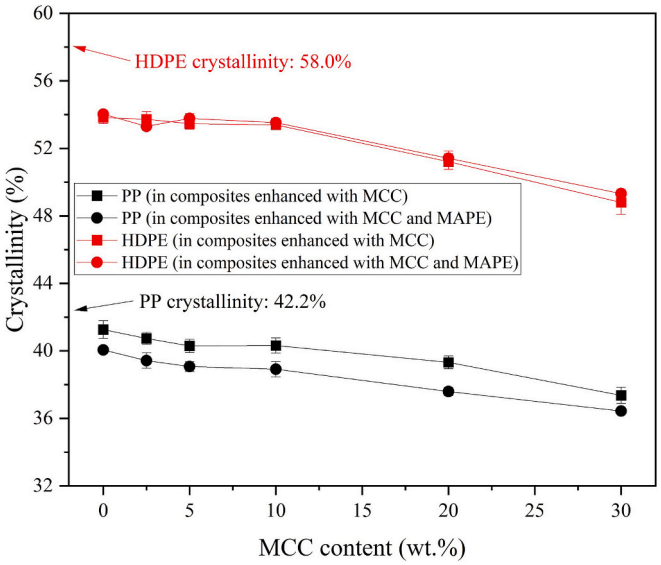

Fig. 8. Crystallinity of PP and HDPE components in the composites.

The introduction of MAPE did not affect HDPE's Xc in either the PP/HDPE blend or the MCC-enhanced composites. However, MAPE slightly decreased PP's Xc in both systems. This reduction is attributed to MAPE enhancing the compatibility between MCC and the polymer matrix, which further restricted the chain mobility of the PP phase, hindering its crystallization. For HDPE, MAPE's PE backbone is highly miscible with HDPE chains, facilitating better chain alignment, as observed in SEM results. This enhanced alignment counteracted the restriction in chain movement caused by improved compatibility, thereby maintaining

HDPE's crystallinity.

3.4. Rheological properties

3.4.1. Complex viscosity

Rheological behaviors were measured to understand the processibility and molecular interactions in the melt state of the composites. Complex viscosity plots are shown in Fig. 9. Compared to the PP/HDPE blend, the addition of MCC particles increased complex viscosity, as the rigid MCC particles restricted polymer chain mobility, enhancing resistance to deformation. For MCC contents between 2.5 and 10 wt%, the complex viscosity remained relatively unchanged, indicating that the dispersed MCC particles had minimal impact on the overall flow behavior. However, when MCC content exceeded 20 wt%, viscosity increased significantly. At higher MCC concentrations, particle–particle interactions intensified, leading to the formation of network structures or agglomerates, which disrupted the continuity of the polymer matrix. This transition resulted in the formation of a percolation network, causing a sharp rise in flow resistance and potentially posing processing challenges for conventional techniques such as extrusion and injection molding.

With the addition of MAPE, the complex viscosity of the composites remained comparable at low MCC content (2.5–10 wt%). However, at high MCC content (20 and 30 wt%), the complex viscosity was significantly lower than that of the composites enhanced with MCC alone. This reduction benefited from the lubricating effect and improved compatibilization provided by MAPE. MAPE encapsulated MCC particles and acted as molecular lubricants at the MCC-polymer interface, reducing interfacial friction caused by direct particle–particle interactions and facilitating deformation [75]. Additionally, MAPE enhanced interfacial adhesion, minimized MCC agglomeration, and suppressed the formation of rigid percolated networks, leading to lower resistance to deformation and improved processability.

The Cross model was employed to quantitatively analyze the flow behaviors of PP/HDPE blend and its composites, and the results are shown in Table 1. The mathematical expression of this empirical equation is as below [76]:

$$\eta^* = \frac{\eta_0}{(1+\lambda\omega)^{1-n}}$$

Table 1
Rheological parameters fitted by the Cross model.

Name	Zero-shear viscosity (η_0, Pa·s)	Characteristic time (λ, s)	Power-law index (n)	Coefficient of determination (R^2)
PP/HDPE	2153	12.9	0.75	0.9962
PP/HDPE + 2.5MCC	2734	21.4	0.77	0.9941
PP/HDPE + 5MCC	2781	26.2	0.77	0.9949
PP/HDPE + 10MCC	2997	26.2	0.77	0.9945
PP/HDPE + 20MCC	22,399	90	0.60	0.9700
PP/HDPE + 30MCC	373,618	142	0.42	0.9760
PP/HDPE + 5MAPE	2678	54.7	0.80	0.9854
PP/HDPE + 5MAPE + 2.5MCC	2628	23.6	0.79	0.9906
PP/HDPE + 5MAPE + 5MCC	2715	24.4	0.78	0.9882
PP/HDPE + 5MAPE + 10MCC	2794	25.3	0.79	0.9922
PP/HDPE + 5MAPE + 20MCC	14,117	87	0.65	0.9966
PP/HDPE + 5MAPE + 30MCC	74,075	147	0.53	0.9991

where η_0 is zero shear viscosity, representing the viscosity at very low shear rates; λ is the characteristic time scale, associated with polymer chain relaxation time, and n is the flow index, indicating the degree of

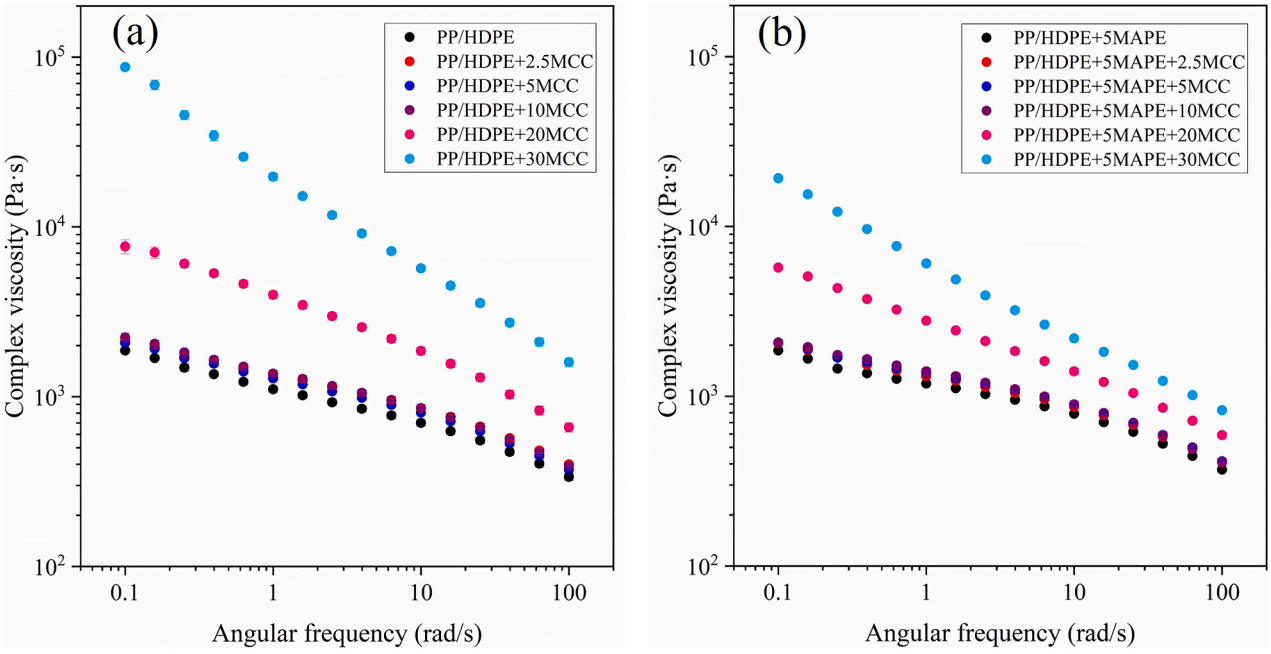

Fig. 9. Plots of complex viscosity for PP/HDPE blends enhanced with (a) MCC and (b) MCC and 5 wt% MAPE.

shear-thinning.

The change in η_0 followed the trend of complex viscosity, with significant increases observed in composites with high MCC content and subsequently decreasing with the addition of MAPE. The λ increased with increasing MCC content as MCC particles constrained polymer chain movement, slowing the relaxation process. However, the influence of MAPE on λ was unclear. The composites with 2.5–10 wt% MCC exhibited a flow index comparable to that of the PP/HDPE blend, while those with high MCC content showed a decreased flow index, indicating more pronounced shear-thinning behavior at high MCC content as shear rate increased. This enhanced flow inconsistency increases the risk of uneven dispersion, potentially leading to structural defects in the final composite.

3.4.2. Storage and loss modulus

Storage and loss modulus plots are presented in Fig. 10. The incorporation of MCC particles led to increases in storage modulus, with more pronounced enhancements at high MCC contents (>20 wt%). These increases are attributed to the intrinsic stiffness of MCC, particularly at high contents, where the polymer matrix became less continuous, and the load-bearing capacity was predominantly governed by the percolated MCC network. After compatibilization with MAPE, the difference in storage modulus between the PP/HDPE blend and its enhanced composites with 2.5–10 wt% MCC became less pronounced, while at 20 and 30 wt% MCC, the storage modulus dramatically decreased compared to the composites enhanced with MCC alone. This is attributed to the lubricating effect and improved MCC dispersion facilitated by MAPE, as previously discussed, leading to increased flexibility within the composites.

A similar trend was observed in the loss modulus results. The addition of MCC at low contents (<10 wt%) did not substantially alter the loss modulus. However, at high MCC content, the loss modulus increased as more energy was required to overcome the heightened frictional resistance caused by increased particle–particle hindrances within the matrix. The presence of MAPE reduced this friction, facilitating smoother deformation and consequently lowering energy dissipation.

3.4.3. Creep-recovery behaviors

The creep-recovery curves in Fig. 11 more clearly illustrate the

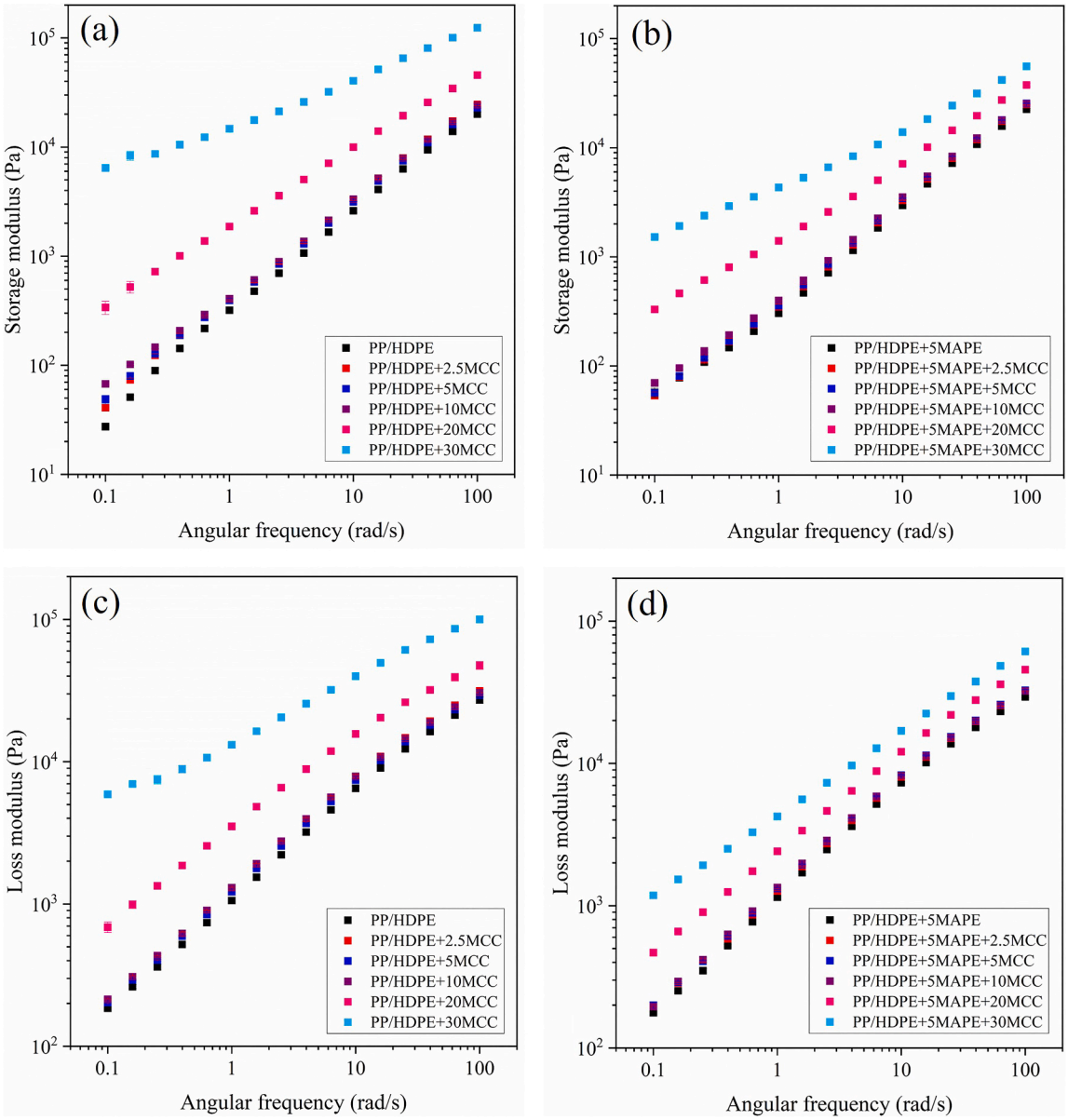

Fig. 10. Plots of storage and loss modulus for PP/HDPE blends enhanced with (a, c) MCC and (b, d) MCC and 5 wt% MAPE.

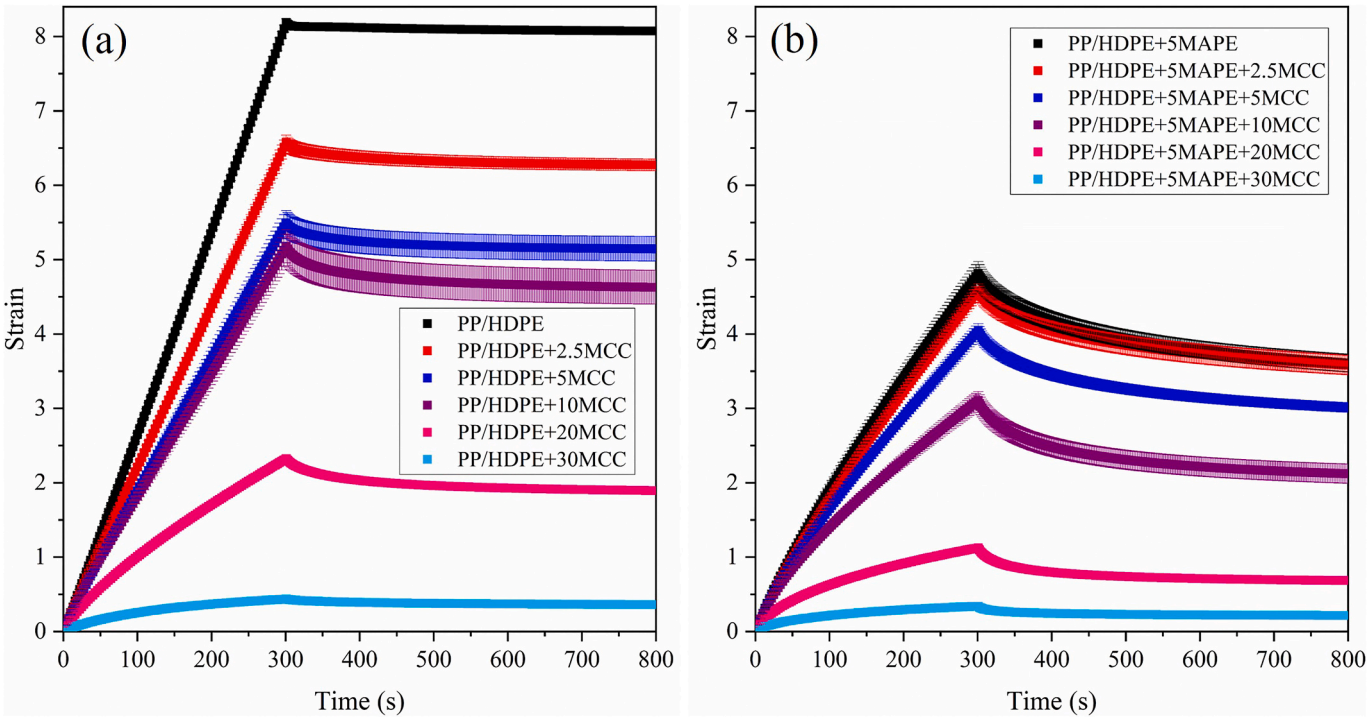

Fig. 11. Creep-recovery behaviors of PP/HDPE blends enhanced with (a) MCC and (b) MCC and 5 wt% MAPE.

changes in stiffness and elasticity of the composites. During the creep stage, the addition of 2.5 wt% MCC to the PP/HDPE blend improved creep resistance, as evidenced by a smaller strain increase over time, indicating higher stiffness. As MCC content increased, stiffness continued to improve due to the restricted mobility of the polymer matrix, resulting in greater structural rigidity. After MAPE compatibilization, creep resistance was further enhanced across all MCC contents, as MAPE strengthened interfacial interactions, improving stress transfer and reducing deformation under sustained load.

During the recovery stage, the PP/HDPE blend exhibited minimal recovery (1.41 %), indicating its predominantly viscous behavior and tendency toward permanent deformation. After incorporating MCC particles, recovery improved with increasing MCC content, reaching 4.63, 6.38, 10.6, and 18.5 % for 2.5, 5, 10, and 20 wt% MCC, respectively. However, at 30 wt% MCC, recovery slightly declined to 17.2 %, likely due to agglomeration, which hindered stress transfer and limited elastic recovery. With MAPE compatibilization, the improved interfacial bonding further contributed to increased elasticity, resulting in recoveries of 21.9, 25.6, 31.7, and 39.1 % for 2.5, 5, 10, and 20 wt% MCC, respectively, despite a slight decline to 36.4 % at 30 wt% MCC.

4. Conclusions

This study examined the mechanical, morphological, thermal, and rheological properties of PP/HDPE blends enhanced with MCC particles and MAPE as a compatibilizer. The results demonstrated that the synergistic effect of MCC and MAPE led to the formation of core–shell structures, where MCC served as the core and MAPE, being miscible with HDPE, formed the shell at the interface. This structure enhanced interfacial interactions between MCC and the PP/HDPE matrix, thereby enhancing mechanical performance. Moreover, thermal analyses revealed that MCC acted as a nucleating agent for PP, while MAPE compatibilization isolated this nucleation by encapsulating MCC. Rheological behaviors discussed the processibility and molecular interactions of the composites. This study proved that MCC particles are promising candidates for valorizing mixed plastic waste.

CRediT authorship contribution statement

Ke Zhan: Writing – review & editing, Writing – original draft, Methodology, Investigation, Formal analysis, Data curation, Conceptualization. **Yucheng Peng:** Writing – review & editing, Supervision, Investigation, Funding acquisition, Conceptualization. **Thomas Elder:** Writing – review & editing.

Declaration of competing interest

The authors declare that they have no known competing financial interests or personal relationships that could have appeared to influence the work reported in this paper.

Acknowledgements

This study is financially supported by the College of Forestry, Wildlife and Environment of Auburn University, the USDA National Institute of Food and Agriculture (McIntire Stennis project ALAZ00079), and the National Science Foundation (2132093). We acknowledge Dr. Douglas J. Gardner and Mr. Justin Crouse for their assistance in measuring the particle size distribution of the MCC.

Data availability

Data will be made available on request.

References

[1] Pottinger AS, Geyer R, Biyani N, Martinez CC, Nathan N, Morse MR, et al. Pathways to reduce global plastic waste mismanagement and greenhouse gas emissions by 2050. Science 2024;386(6726):1168–73.
[2] Geyer R, Jambeck JR, Law KL. Production, use, and fate of all plastics ever made. Sci Adv 2017;3(7):e1700782.
[3] Jehanno C, Alty JW, Roosen M, De Meester S, Dove AP, Chen EYX, et al. Critical advances and future opportunities in upcycling commodity polymers. Nature 2022;603(7903):803–14.
[4] Dai L, Lata S, Cobb K, Zou R, Lei H, Chen P, et al. Recent advances in polyolefinic plastic pyrolysis to produce fuels and chemicals. J Anal Appl Pyrol 2024;180:106551.

[5] Zhou X, He P, Peng W, Zhou J, Jiang M, Zhang H, et al. A value-added and carbon-reduction approach to upcycle mixed plastic waste into methane and carbon microspheres. Resour Conserv Recycl 2023;193:106988.
[6] Jin K, Vozka P, Gentilcore C, Kilaz G, Wang N-H-L. Low-pressure hydrothermal processing of mixed polyolefin wastes into clean fuels. Fuel 2021;294:120505.
[7] Xu J, Eagan JM, Kim S-S, Pan S, Lee B, Klimovica K, et al. Compatibilization of isotactic polypropylene (iPP) and high-density polyethylene (HDPE) with iPP–PE multiblock copolymers. Macromolecules 2018;51(21):8585–96.
[8] Subhani HA, Khushnood RA, Shakeel S. Synthesis of recycled bricks containing mixed plastic waste and foundry sand: physico-mechanical investigation. Constr Build Mater 2024;416:135197.
[9] Singh N, Walker TR. Plastic recycling: a panacea or environmental pollution problem. npj Materials Sustainability 2024;2(1):17.
[10] Chu M, Tu W, Yang S, Zhang C, Li Q, Zhang Q, et al. Sustainable chemical upcycling of waste polyolefins by heterogeneous catalysis. SusMat 2022;2(2):161–85.
[11] Miao Y, Zhao Y, Waterhouse GIN, Shi R, Wu L-Z, Zhang T. Photothermal recycling of waste polyolefin plastics into liquid fuels with high selectivity under solvent-free conditions. Nat Commun 2023;14(1):4242.
[12] Li X, Mahadas NA, Zhang M, DePodesta J, Stefik M, Tang C. Sustainable high-density polyethylene via chemical recycling: from modification to polymerization methods. Polymer 2024;295:126698.
[13] Karaagac E, Koch T, Archodoulaki V. Choosing an effective compatibilizer for a virgin HDPE rich-HDPE/PP model blend. Polymers 2021;13:3567.
[14] Jubinville D, Esmizadeh E, Saikrishnan S, Tzoganakis C, Mekonnen T. A comprehensive review of global production and recycling methods of polyolefin (PO) based products and their post-recycling applications. Sustain Mater Technol 2020;25:e00188.
[15] Thiounn T, Smith RC. Advances and approaches for chemical recycling of plastic waste. J Polym Sci 2020;58(10):1347–64.
[16] Sullivan KP, Werner AZ, Ramirez KJ, Ellis LD, Bussard JR, Black BA, et al. Mixed plastics waste valorization through tandem chemical oxidation and biological funneling. Science 2022;378(6616):207–11.
[17] Aumnate C, Rudolph N, Sarmadi M. Recycling of polypropylene/polyethylene blends: effect of chain structure on the crystallization behaviors. Polymers 2019;11(9):1456.
[18] Klimovica K, Pan S, Lin TW, Peng X, Ellison CJ, LaPointe AM, et al. Compatibilization of iPP/HDPE blends with PE-g-iPP graft copolymers. ACS Macro Lett 2020;9(8):1161–6.
[19] Saleem J, Khalid Baig MZ, Shahid UB, Luque R, McKay G. Mixed plastics waste valorization to high-added value products via thermally induced phase separation and spin-casting. Green Energy Environ 2024;9(10):1627–40.
[20] Stewart KME, Stonecipher E, Ning H, Pillay SB. Mixing rules for high density polyethylene-polypropylene blends. Can J Chem Eng 2023;101(9):5395–407.
[21] Lin J-H, Pan Y-J, Liu C-F, Huang C-L, Hsieh C-T, Chen C-K, et al. Preparation and compatibility evaluation of polypropylene/high density polyethylene polyblends. Materials 2015;8(12):8850–9.
[22] Bartlett DW, Barlow JW, Paul DR. Mechanical properties of blends containing HDPE and pp. J Appl Polym Sci 1982;27(7):2351–60.
[23] Chiu F-C, Yen H-Z, Lee C-E. Characterization of PP/HDPE blend-based nanocomposites using different maleated polyolefins as compatibilizers. Polym Test 2010;29(3):397–406.
[24] Verberckmoes A, Fernandez E, Martins C, Reyes P, Cardon L, D'Hooge DR, et al. Morphological analysis of mechanically recycled blends of high density polyethylene and polypropylene with strong difference in melt flow index. Polymer 2024;300:126999.
[25] Graziano A, Jaffer S, Sain M. Review on modification strategies of polyethylene/polypropylene immiscible thermoplastic polymer blends for enhancing their mechanical behavior. J Elastomers Plast 2018;51(4):291–336.
[26] Wolff P, Dickert A, Kretschmer WP, Kempe R. iPP/PE multiblock copolymers for plastic blend recycling synthesized by coordinative chain transfer polymerization. Macromolecules 2022;55(15):6435–42.
[27] Carmeli E, Fenni SE, Caputo MR, Müller AJ, Tranchida D, Cavallo D. Surface nucleation of dispersed polyethylene droplets in immiscible blends revealed by polypropylene matrix self-nucleation. Macromolecules 2021;54(19):9100–12.
[28] Huang DE, Kotula AP, Snyder CR, Migler KB. Crystallization kinetics in an immiscible polyolefin blend. Macromolecules 2022;55(24):10921–32.
[29] Khabbaz HS, Demets R, Gahleitner M, Duscher B, Stam R, Dimitrova A, et al. Rheological insights into the degradation behavior of PP/HDPE blends. Polym Degrad Stab 2024.
[30] Wang G, Dong M, Yuan M, Ren J, Gu J, Zhang X, et al. Effects of process conditions and nano-fillers on the cell structure and mechanical properties of co-injection molded polypropylene-polyethylene composites. Polymer 2024;299:126935.
[31] Kruszynski J, Nowicka W, Rozanski A, Liu Y, Parisi D, Yang L, et al. iPP/HDPE blends compatibilized by a polyester: an unconventional concept to valuable products. Sci Adv 2024;10(21).
[32] Ruiz de Ballesteros O, Rispo A, Femina G, Davide S, Nocella F, Romano R, et al. Compatibilization of isotactic polypropylene (iPP) and polyethylene (PE) with PP-based olefin block copolymers. Polymer 2025;319:128040.
[33] Souza AMC, Demarquette NR. Influence of coalescence and interfacial tension on the morphology of PP/HDPE compatibilized blends. Polymer 2002;43(14):3959–67.
[34] Dikobe DG, Luyt AS. Thermal and mechanical properties of PP/HDPE/wood powder and MAPP/HDPE/wood powder polymer blend composites. Thermochim Acta 2017;654:40–50.
[35] Schyns ZOG, Shaver MP. Mechanical recycling of packaging plastics: a review. Macromol Rapid Commun 2021;42(3):2000415.
[36] Rudin JWTaA. A review of polyethylene- polypropylene blends and their compatibilization. Adv Polym Tech 1994;13(1).
[37] Graziano A, Titton Dias OA, Sena Maia B, Li J. Enhancing the mechanical, morphological, and rheological behavior of polyethylene/polypropylene blends with maleic anhydride-grafted polyethylene. Polym Eng Sci 2021;61(10):2487–95.
[38] Yokoyama K, Guan Z. A Vitrimer acts as a compatibilizer for polyethylene and polypropylene blends. Angew Chem Int Ed 2024;63(20):e202317264.
[39] González J, Albano C, Ichazo M, Díaz B. Effects of coupling agents on mechanical and morphological behavior of the PP/HDPE blend with two different CaCO3. Eur Polym J 2002;38(12):2465–75.
[40] Ragaert K, Huysveld S, Vyncke G, Hubo S, Veelaert L, Dewulf J, et al. Design from recycling: a complex mixed plastic waste case study. Resour Conserv Recycl 2020;155:104646.
[41] Eagan JM, Xu J, Di Girolamo R, Thurber CM, Macosko CW, LaPointe AM, et al. Combining polyethylene and polypropylene: enhanced performance with PE/iPP multiblock polymers. Science 2017;355(6327):814–6.
[42] Radonjić G, Gubeljak N. The use of ethylene/propylene copolymers as compatibilizers for recycled polyolefin blends. Macromol Mater Eng 2002;287(2):122–32.
[43] Parameswaranpillai J, Pulikkalparambil H, Sanjay MR, Siengchin S. Polypropylene/high-density polyethylene based blends and nanocomposites with improved toughness. Mater Res Express 2019;6(7):075334.
[44] Choudhary V, Varma HS, Varma IK. Effect of EPDM rubber on melt rheology, morphology and mechanical properties of polypropylene/HDPE (9010) blend. 2. Polymer 1991;32(14):2541–5.
[45] Karaagac E, Koch T, Archodoulaki V-M. The effect of PP contamination in recycled high-density polyethylene (rPE-HD) from post-consumer bottle waste and their compatibilization with olefin block copolymer (OBC). Waste Manag 2021;119:285–94.
[46] Ahmad Ramazani SA, Abdi Valami M, Khak M. Effect of poly (propylene-g-maleic anhydride) on the morphological, rheological, and mechanical properties of PP/HDPE blend. J Thermoplast Compos Mater 2009;22(5):519–30.
[47] Wang Y, Shi Y, Shao W, Ren Y, Dong W, Zhang F, et al. Crystallization, structures, and properties of different polyolefins with similar grafting degree of maleic anhydride. Polymers 2020;12(3).
[48] Fang C, Nie L, Liu S, Yu R, An N, Li S. Characterization of polypropylene–polyethylene blends made of waste materials with compatibilizer and nano-filler. Compos B Eng 2013;55:498–505.
[49] Ha C-S, Park H-D, Kim Y, Kwon S-K, Cho W-J. Compatibilizer in polymer blends for the recycling of plastics waste I: preliminary studies on 50/50 wt% virgin polyblends. Polym Adv Technol 1996;7(5–6):483–92.
[50] Clemons C. Elastomer modified polypropylene–polyethylene blends as matrices for wood flour–plastic composites. Compos A Appl Sci Manuf 2010;41(11):1559–69.
[51] Zhan K, Elder T, Peng Y. Enhancing polypropylene/polyethylene blend performance through compatibilization for a sustainable future: a mini review focusing on establishing bio-derived filler based hybrid compatibilizer system. Macromol Rapid Commun 2024:2400724.
[52] Ramachandran A, George KE, George TS, Krishnan A. Optimisation of processing conditions of PP/HDPE/nano kaolinite clay composites by response surface methodology. Int J Plast Technol 2012;16(2):136–49.
[53] Hammache Y, Serier A, Chaoui S. The effect of thermoplastic starch on the properties of polypropylene/high density polyethylene blend reinforced by nano-clay. Mater Res Express 2020;7(2):025308.
[54] Anjana R, Krishnan AK, Goerge TS, George KE. Design of experiments for thermo-mechanical behavior of polypropylene/high-density polyethylene/nanokaolinite clay composites. Polym Bull 2014;71(2):315–35.
[55] Navarro CU, Parra C, Albano C, González J. Composites of PP/HDPE- CaCO3: crystallinity and morphology using virgin and recycled HDPE. Microsc Microanal 2003;9(S02):16–7.
[56] Gao H, Xie Y, Ou R, Wang Q. Grafting effects of polypropylene/polyethylene blends with maleic anhydride on the properties of the resulting wood–plastic composites. Compos A Appl Sci Manuf 2012;43(1):150–7.
[57] Gao H, Song Y-m, Wang Q-w, Han Z, Zhang M-l. Rheological and mechanical properties of wood fiber-PP/PE blend composites. J For Res 2008;19(4):315–8.
[58] Clemons CM, Sabo RC, Kaland ML, Hirth KC. Effects of silane on the properties of wood-plastic composites with polyethylene-polypropylene blends as matrices. J Appl Polym Sci 2011;119(3):1398–409.
[59] Bagheriasl D, Carreau PJ, Dubois C, Riedl B. Properties of polypropylene and polypropylene/poly(ethylene-co-vinyl alcohol) blend/CNC nanocomposites. Compos Sci Technol 2015;117:357–63.
[60] Wang X, Wang P, Liu S, Zhan K, Via B, Gallagher T, et al. Identification of percolation threshold of spray-dried cellulose nanocrystals in homopolymer polypropylene composites. J Appl Polym Sci 2024;141(28).
[61] Peng Y, Gallegos SA, Gardner DJ, Han Y, Cai Z. Maleic anhydride polypropylene modified cellulose nanofibril polypropylene nanocomposites with enhanced impact strength. Polym Compos 2016;37(3):782–93.
[62] Saidmuhamedova MQ, Turdiqulov IH, Atakhanov AA, Ashurov NS, Abdurazakov M, Rashidova SSR, et al. Biodegradable polyethylene-based composites filled with cellulose micro- and nanoparticles. Eurasian J Chem 2023;110(2):94–106.
[63] Izzati Zulkifli N, Samat N, Anuar H, Zainuddin N. Mechanical properties and failure modes of recycled polypropylene/microcrystalline cellulose composites. Mater Des 2015;69:114–23.

[64] Spoljaric S, Genovese A, Shanks RA. Polypropylene–microcrystalline cellulose composites with enhanced compatibility and properties. Compos A Appl Sci Manuf 2009;40(6–7):791–9.
[65] Xiuju Z, Juncai S, Huajun Y, Zhidan L, Shaozao T. Mechanical properties, morphology, thermal performance, crystallization behavior, and kinetics of pp/microcrystal cellulose composites compatibilized by two different compatibilizers. J Thermoplast Compos Mater 2011;24(6):735–54.
[66] Kong Y, Hay JN. The measurement of the crystallinity of polymers by DSC. Polymer 2002;43(14):3873–8.
[67] Rodríguez-Liébana JA, Martín-Lara MA, Navas-Martos FJ, Peñas-Sanjuan A, Godoy V, Arjandas S, et al. Morpho-structural and thermo-mechanical characterization of recycled polypropylene and polystyrene from mixed post-consumer plastic waste. J Environ Chem Eng 2022;10(5):108332.
[68] Barone JR. Polyethylene/keratin fiber composites with varying polyethylene crystallinity. Compos A Appl Sci Manuf 2005;36(11):1518–24.
[69] Spoljaric S, Genovese A, Shanks RA. Polypropylene–microcrystalline cellulose composites with enhanced compatibility and properties. Compos A Appl Sci Manuf 2009;40(6):791–9.
[70] Clemons CM, Caulfield DF, Giacomin AJ. Dynamic fracture toughness of cellulose-fiber-reinforced polypropylene: preliminary investigation of microstructural effects. J Elastomers Plast 1999;31(4):367–78.
[71] Fenni SE, Müller AJ, Cavallo D. Understanding polymer nucleation by studying droplets crystallization in immiscible polymer blends. Polymer 2023;264:125514.
[72] Gesztelyi R, Zsuga J, Kemeny-Beke A, Varga B, Juhasz B, Tosaki A. The Hill equation and the origin of quantitative pharmacology. Arch Hist Exact Sci 2012;66(4):427–38.
[73] Goutelle S, Maurin M, Rougier F, Barbaut X, Bourguignon L, Ducher M, et al. The Hill equation: a review of its capabilities in pharmacological modelling. Fundam Clin Pharmacol 2009;22:633–48.
[74] Mohan Bhasney S, Kumar A, Katiyar V. Microcrystalline cellulose, polylactic acid and polypropylene biocomposites and its morphological, mechanical, thermal and rheological properties. Compos B Eng 2020;184:107717.
[75] Wang L, Gardner DJ, Bousfield DW. Cellulose nanofibril-reinforced polypropylene composites for material extrusion: rheological properties. Polym Eng Sci 2018;58(5):793–801.
[76] Zhan K, Meadows D, Levy L, Hou R, Rahman T, Davis V, et al. Impact of thermomechanical reprocessing on multilayer plastic packaging blend. Polym Degrad Stab 2024;222:110710.